

# **NUMERICAL MODELING OF UNSTEADY THERMOFLUID DYNAMICS IN CRYOGENIC SYSTEMS**

**Alok Majumdar**

NASA/Marshall Space Flight Center  
Huntsville, Alabama

## **ABSTRACT**

This paper describes a finite volume procedure for network flow analysis of unsteady thermofluid dynamics in cryogenic systems. A flow network is defined as a system of fluid nodes connected in series or parallel mode by branches. The mass, energy and specie conservation equations are solved at the nodes in conjunction with the thermodynamic equation of state for a real fluid. An upwind scheme is used to compute transport of energy and specie from neighboring nodes. The momentum conservation equation is solved at the branches. Fluid is modeled as compressible fluid irrespective of its state. The governing equations are solved by a hybrid numerical technique that is a combination of simultaneous and successive substitution method. Two examples of thermofluid transients are described. In the first example, fluid transient after a rapid closing of a valve in a long cryogenic pipeline was calculated and compared with the solution of method of characteristics. In the second example, the chilldown of a long cryogenic pipeline was modeled and compared with experimental results.

## **INTRODUCTION**

Unsteady thermofluid dynamic phenomenon [1] is common in cryogenic systems. They include pressurization and blow down of cryogenic tanks, sudden opening or closing of valves in long pipeline, chilldown of cryogenic transfer line and rocket engines prior to ignition. Development of accurate, robust and economic numerical model is a critical need for design and operation of such systems. This paper describes the progress we have made at Marshall Space Flight Center in recent years to develop this capability using a general-purpose flow network code, Generalized Fluid System Simulation Program (GFSSP).

Thermofluid transients can be categorized into thermodynamic transient and fluid transient. Pressurization and blow down belong to thermodynamic transient while rapid opening or closing of valves (commonly known as water hammer) are classified as fluid transient. Numerical modeling of thermodynamic transient requires the solution of unsteady mass and energy conservation equations while momentum equation is solved in steady state. On the other hand, the modeling of fluid transient requires the solution of unsteady momentum equation in addition to mass and energy equations. Fluid transient problems [2] are typically solved by the method of characteristics (MOC). In the method of characteristics, partial differential equations are transformed into ordinary differential equation using the line of characteristics that are determined from the speed of sound.

While MOC has been found to be accurate in predicting hydraulic transients in long pipeline, its application in complex flow network for cryogenic system is limited.

Commercially available codes, FLUENT [3] and EASY5 [4] are based on finite difference formulation. The present approach [5] is based on finite volume modeling of conservation equations in a fluid system network. For Navier-Stokes analysis, finite volume formulation has been found more robust and flexible than the finite difference and finite element solvers. Figure 1 shows classification of computational fluid dynamics code where GFSSP has been classified as finite volume based network flow analysis code.

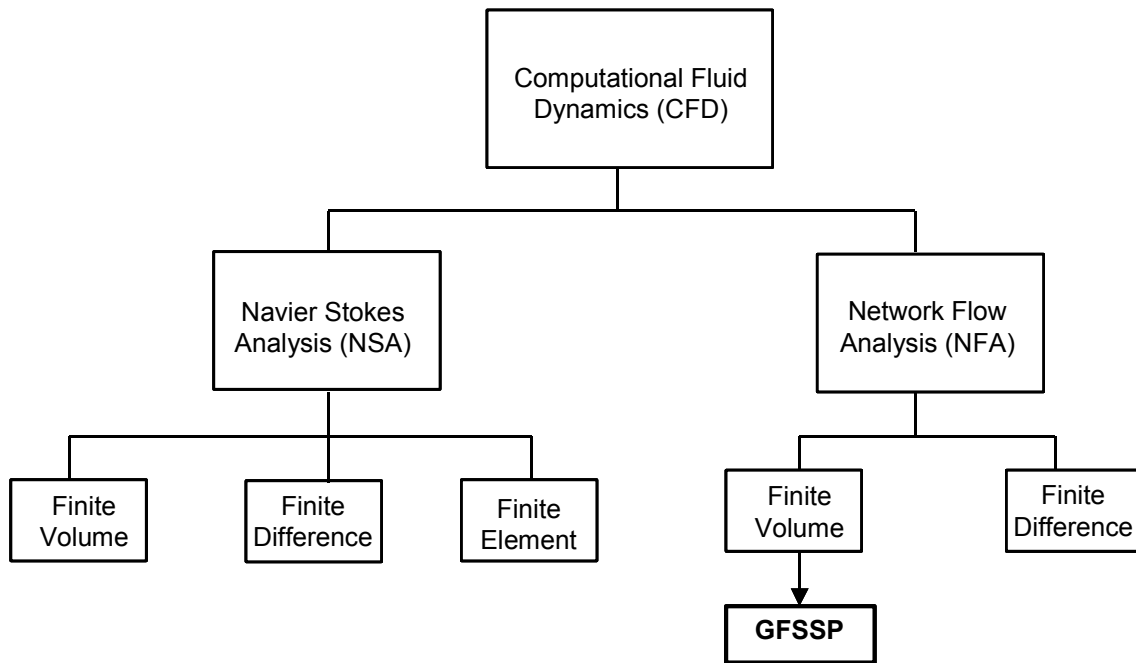


**Figure 1. Classification of CFD Codes**

## **MATHEMATICAL FORMULATION**

Figure 2 shows a typical flow network consisting of nodes and branches. There are two kinds of nodes: boundary and internal nodes. At the boundary nodes, pressure, temperature and concentrations are specified. At the internal nodes, all scalar properties such as pressure, temperature, density, compressibility factor and viscosity are computed. Mass, energy and specie conservation equations are solved at the internal nodes in conjunction with the thermodynamic equation of state for a real fluid. Flowrates are computed at the branches by solving the momentum conservation equation.

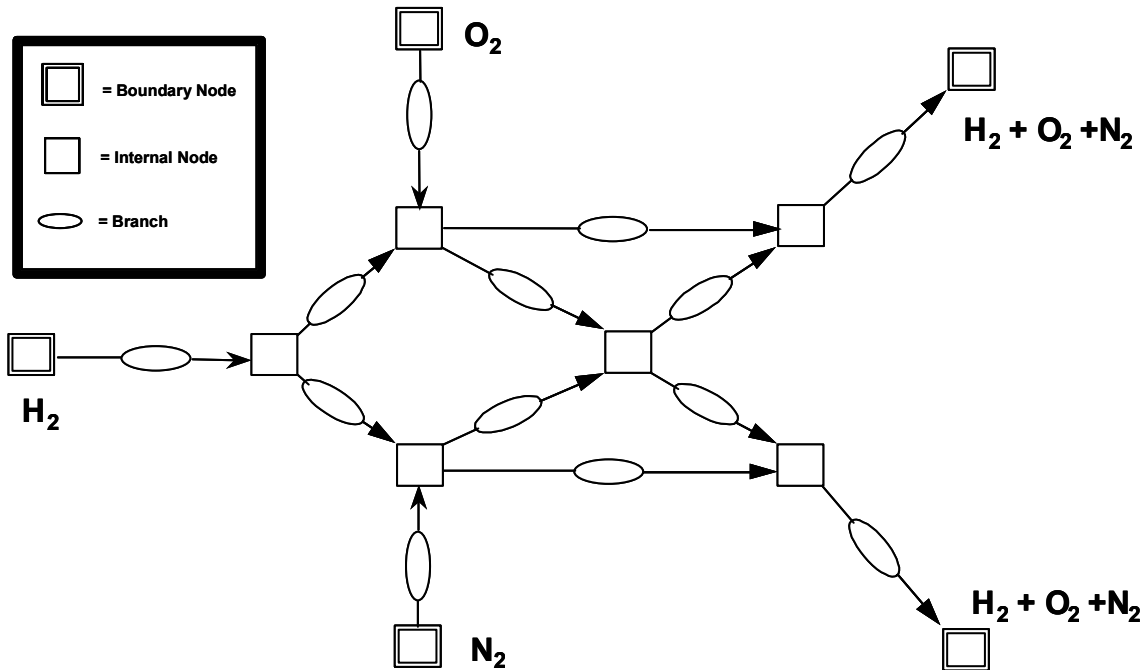


**Figure 2. A flow network consisting of Boundary Nodes, Internal Nodes and Branches**

**Finite Volume Formulation in a Fluid Network**

The finite volume formulation requires governing equations to be expressed in conservative form instead of finite difference or finite element form derived from differential equations of mass, momentum and energy transport. The rate of change of a conserved property in a given control volume is expressed as the vector sum of transported property from neighboring control volumes together with source or sink terms. The unknown variables in the flow circuit of figure 2 are pressure, temperature, concentrations and flowrate. These variables are solved from the equations listed in Table 1.

**Table 1. Mathematical Closure**

<u>Unknown Variables</u>	<u>Equations to Solve</u>
1. Pressure	1. Mass Conservation Equation
2. Flowrate	2. Momentum Conservation Equation
3. Temperature	3. Energy Conservation Equation (First or Second Law of Thermodynamics)
4. Specie Concentrations	4. Conservation Equations for Mass Fraction of Species
5. Mass	5. Thermodynamic Equation of State

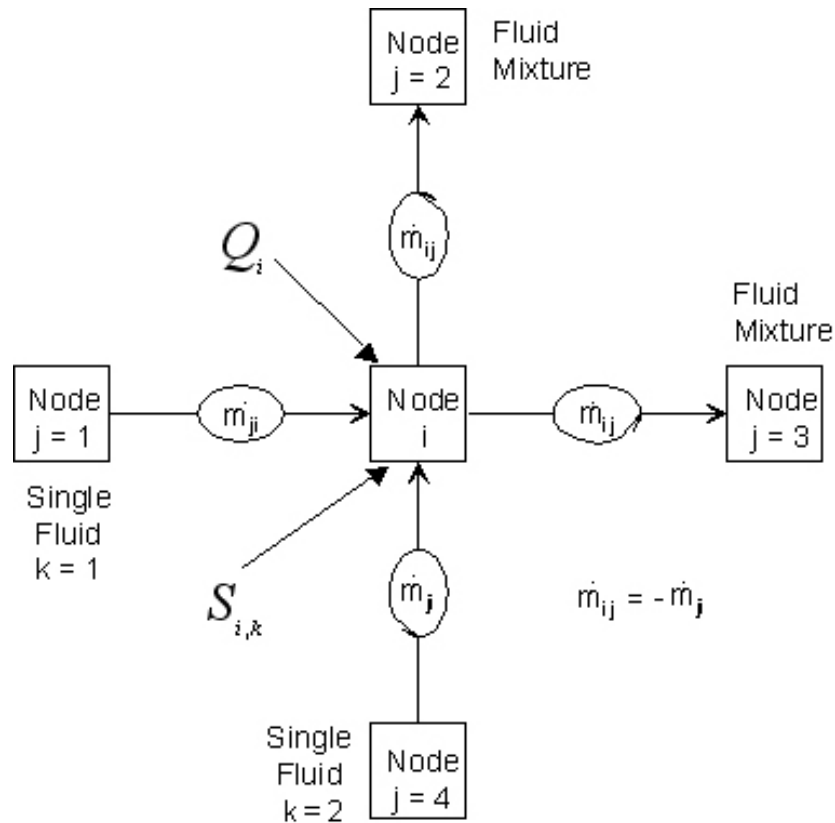


**Figure 3. Schematic of connections between Nodes by Branches and the indexing practice**

Figure 3 shows that Node i is connected with four neighboring nodes ( $j = 1,2,3,4$ ) by four branches. It is possible that two nodes can be connected by two or more branches (parallel connection). There is no limit of number of neighboring nodes connected to a given node. The conservation equations are now described:

### Mass Conservation

The mass conservation equation at the  $i^{\text{th}}$  node can be written as

$$\frac{m_{\tau+\Delta\tau} - m_{\tau}}{\Delta\tau} = - \sum_{j=1}^{j=n} \dot{m}_j \quad (1)$$

Equation 1 implies that the net mass flow from a given node must equate to rate of change of mass in the control volume. In the steady state formulation, the left side of the equation is zero, such that the total mass flow rate into a node is equal to the total mass flow rate out of the node.

## Momentum Conservation

The momentum conservation equation at the ij branch can be written as

$$\frac{(mu)_{\tau+\Delta\tau} - (mu)_{\tau}}{g_c \Delta\tau} + MAX\left|\dot{m}_{ij}, 0\right|(u_{ij} - u_u) - MAX\left|-\dot{m}_{ij}, 0\right|(u_{ij} - u_u) = (p_i - p_j)A_{ij} - K_f \dot{m}_{ij} \left|\dot{m}_{ij}\right| A_{ij} \quad (2)$$

The left hand side of the momentum equation contains unsteady and inertia term. The pressure and friction force appear in the right hand side of the equation. The unsteady term represents rate of change of momentum with time. For steady state flow, time step is set to an arbitrary large value and this term is reduced to zero. The inertia term is important when there is a significant change in velocity in the longitudinal direction due to change in area and density. An upwind differencing scheme is used to compute the velocity differential. The pressure term represents the pressure gradient in the branch. The pressures are located at the upstream and downstream face of a branch. Friction was modeled as a product of  $K_f$  and the square of the flow rate and area. It may be noted that  $\dot{m}_{ij} \left|\dot{m}_{ij}\right|$  has been used instead of  $\dot{m}_{ij}^2$ . Recognizing the flowrate is a vector quantity; this technique is used to ensure that friction always opposes the flow.  $K_f$  is a function of the fluid density in the branch and the nature of the flow passage being modeled by the branch. For a pipe  $K_f$  can be expressed as

$$K_f = \frac{8fL}{\rho_u \pi^2 D^5 g_c} \quad (3)$$

For a valve,  $K_f$  can be expressed as

$$K_f = \frac{1}{2g_c \rho_u C_L^2 A^2} \quad (4)$$

The friction factor,  $f$ , in equation (3) is calculated from Colebrook equation [6], which is expressed as

$$\frac{1}{\sqrt{f}} = -2 \log \left[ \frac{\varepsilon}{3.7D} + \frac{2.51}{\text{Re} \sqrt{f}} \right] \quad (5)$$

## Energy Conservation

The energy conservation equation for node i, shown in Figure 3, can be expressed following the first law of thermodynamics and using enthalpy as the dependant variable. The energy conservation equation based on enthalpy can be written as

$$\begin{aligned} & \frac{m\left(h - \frac{p}{\rho J}\right)_{\tau+\Delta\tau} - m\left(h - \frac{p}{\rho J}\right)_{\tau}}{\Delta\tau} \\ &= \sum_{j=1}^{j=n} \left\{ \text{MAX}\left[-\dot{m}_{ij}, 0\right] h_j - \text{MAX}\left[\dot{m}_{ij}, 0\right] h_i \right\} + \dot{Q}_i, \end{aligned} \quad (6)$$

where

$$\dot{Q}_i = h_c A (T_{\text{solid}} - T_{\text{fluid}}). \quad (6a)$$

The MAX operator represents the upwind formulation [7].  $\dot{Q}_i$  represents solid to fluid heat transfer that will be described in more detail in a following section.

### Equation of State

The resident mass in the  $i^{\text{th}}$  control volume can be expressed from the equation of state for a real fluid as

$$m = \frac{pV}{RTz} \quad (7)$$

For a given pressure and enthalpy the temperature and compressibility factor in equation 6 is determined from the thermodynamic property program developed by Hendricks et al [8,9].

### Gas Liquid Mixture

To model a homogeneous mixture of liquid and gas, the conservation equations for both liquid and gaseous species are solved in conjunction with equations (1), (2) and (7). The conservation equation of  $k^{\text{th}}$  specie can be written as:

$$\frac{(m_i c_{i,k})_{\tau+\Delta\tau} - (m_i c_{i,k})_{\tau}}{\Delta\tau} = \sum_{j=1}^{j=n} \left\{ \text{MAX}\left[-\dot{m}_{ij}, 0\right] c_{j,k} - \text{MAX}\left[\dot{m}_{ij}, 0\right] c_{i,k} \right\} + \dot{S}_{i,k} \quad (8)$$

Unlike a single fluid, the energy equation for gas liquid mixture is expressed in terms of temperature instead of enthalpy:

$$(T_i)_{\tau+\Delta\tau} = \frac{\sum_{j=1}^{j=n} \sum_{k=1}^{k=nf} C_{p_k} x_k T_j \text{MAX}[-m_{ij}, 0] + (C_{v,i} m_i T_i)_{\tau} / \Delta\tau}{\sum_{j=1}^{j=n} \sum_{k=1}^{k=nf} C_{p_k} x_k \text{MAX}[m_{ij}, 0] + (C_{v,i} m)_{\tau} / \Delta\tau} \quad (9)$$

It is assumed that the liquid and gas have the same temperature. However the specific heats of liquid and gas are evaluated from a thermodynamic property program [8,9]. The density, specific heat, and the viscosity of the mixture are then calculated from the following relations:

$$\rho_i = \frac{P_i}{\sum_{k=1}^{k=nf} [\bar{x}_k R_k]} \sum_{k=1}^{k=nf} [\bar{x}_k z_k] T_i \quad (10)$$

where,

$$z_k = \frac{P_i}{\rho_k R_k T_i} \quad (11)$$

$$C_v = \frac{\sum_{k=1}^{k=nf} \bar{x}_k C_{v,k} M_k}{\sum_{k=1}^{k=nf} \bar{x}_k M_k} \quad (12)$$

$$\mu_i = \sum_{k=1}^{k=nf} \bar{x}_k \mu_k \quad (13)$$

## Phase Change

Modeling phase change is fairly straightforward in the present formulation. The vapor quality of saturated liquid vapor mixture is calculated from:

$$x_v = \frac{h - h_f}{h_g - h_f} \quad (14)$$

Assuming a homogeneous mixture of liquid and vapor, the density, specific heat and viscosity are computed from the following:

$$\phi = (1 - x_v) \phi_l + x_v \phi_v \quad (15)$$

where  $\phi$  represents density, specific heat or viscosity.

## Solid-to-Fluid Heat Transfer

Each internal fluid node is connected with a solid node as shown in Figure 2. The energy conservation equation for the solid node is solved in conjunction with all other conservation equations. The energy conservation equation for the solid can be expressed as

$$\frac{(mC_p T_{\text{solid}})_{\tau+\Delta\tau} - (mC_p T_{\text{solid}})_{\tau}}{\Delta\tau} = -h_c A (T_{\text{solid}} - T_{\text{fluid}}). \quad (16)$$

The heat transfer coefficient of Eq. (10) is computed from the correlation given by Miropolskii: [10]

$$Nu = \frac{h_c D}{k_v}, \quad (17)$$

where

$$Nu = 0.023 (Re_{\text{mix}})^{0.8} (Pr_v)^{0.4} (Y), \quad (18)$$

$$Re_{\text{mix}} = (\rho u D / \mu_v) [x + (\rho_v / \rho_l)(1 - x)], \quad (19)$$

$$Pr_v = (C_p \mu_v / k_v), \quad (20)$$

and

$$Y = 1 - 0.1 \left( \frac{\rho_v}{\rho_l} - 1 \right)^{0.4} (1 - x)^{0.4}. \quad (21)$$

## SOLUTION PROCEDURE

The pressure, enthalpy, and resident mass in internal nodes and flowrate in branches are calculated by solving equations (1), (6), (7), and (2) respectively. For a mixture, the conservation of species equation (8) is solved in conjunction with equations (1), (7) and (2). The energy equation is solved in terms of temperature (9) instead of enthalpy. A combination of the Newton-Raphson method and the successive substitution method has been used to solve the set of equations. The mass conservation (2), momentum conservation (3) and resident mass (7) equations are solved by the Newton-Raphson method. The energy and specie conservation equations are solved by the successive substitution method. The temperature, density and viscosity are computed from pressure and enthalpy using a thermodynamic property program (8,9). Figure 3 shows the flow diagram of the Simultaneous Adjustment with Successive Substitution (SASS) scheme. The iterative cycle is terminated when the normalized maximum correction  $\Delta_{\text{max}}$  is less than the convergence criterion  $C_c$ .  $\Delta_{\text{max}}$  is determined from

$$\Delta_{\max} = \max \left| \sum_{i=1}^{N_E} \frac{\phi_i'}{\phi_i} \right| \quad (16)$$

The convergence criterion is set to 0.001 for all models presented in this paper. The details of the numerical procedure are described in Reference 4.

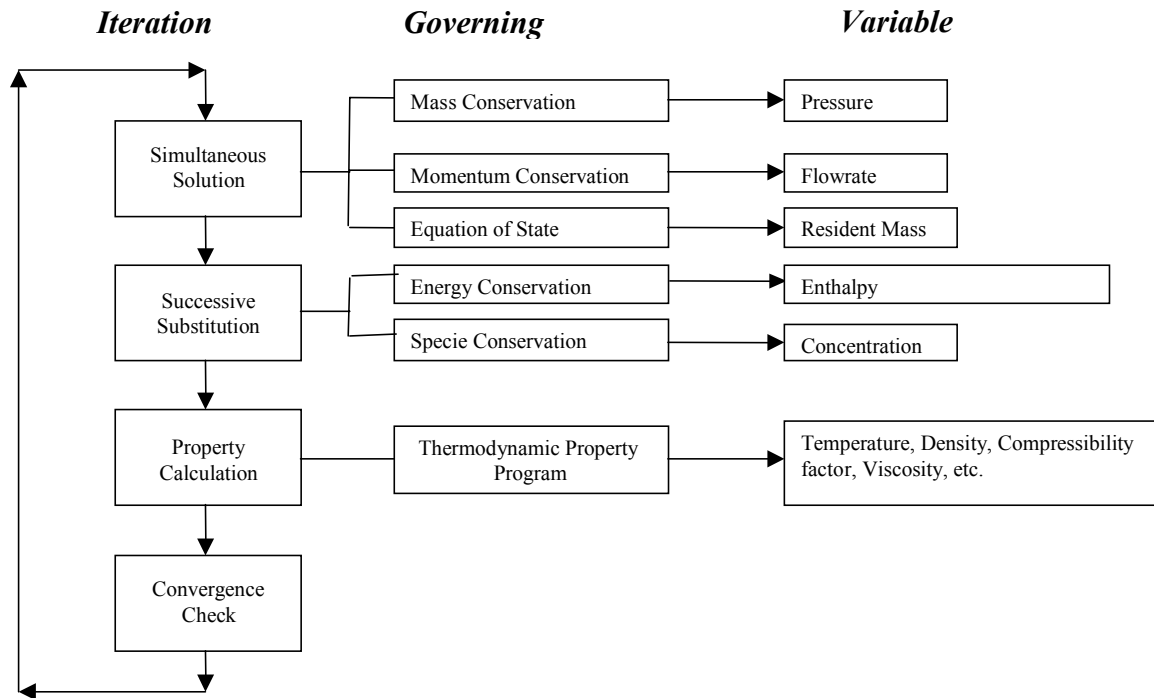


**Figure 4. SASS (Simultaneous Adjustment with Successive Substitution) Scheme for solving Governing Equations**

## COMPUTER PROGRAM

GFSSP (Generalized Fluid System Simulation Program) embodies the mathematical formulation and solution procedure described in the previous sections. The program structure is shown in Figure 5. The program consists of three modules: Graphical User Interface, Solver and User Subroutines. VTASC (Visual Thermofluid dynamics Analyzer for Systems & Components) is the Graphical User Interface (GUI). VTASC allows user to create a flow circuit using a point and click paradigm. It creates an ASCII data file that is read by the solver module and reads the output data file for post processing the results. Figure 6 shows a VTASC window with a model of a rapid valve closure in a long pipeline. The pressure transient at the valve upstream is shown plotted along with the model. The solver module reads the data file generated by VTASC. It generates all governing equations from network data. The equations are solved by the iterative algorithm (SASS). It calls thermodynamic property programs to obtain the necessary properties during the iterative cycle.

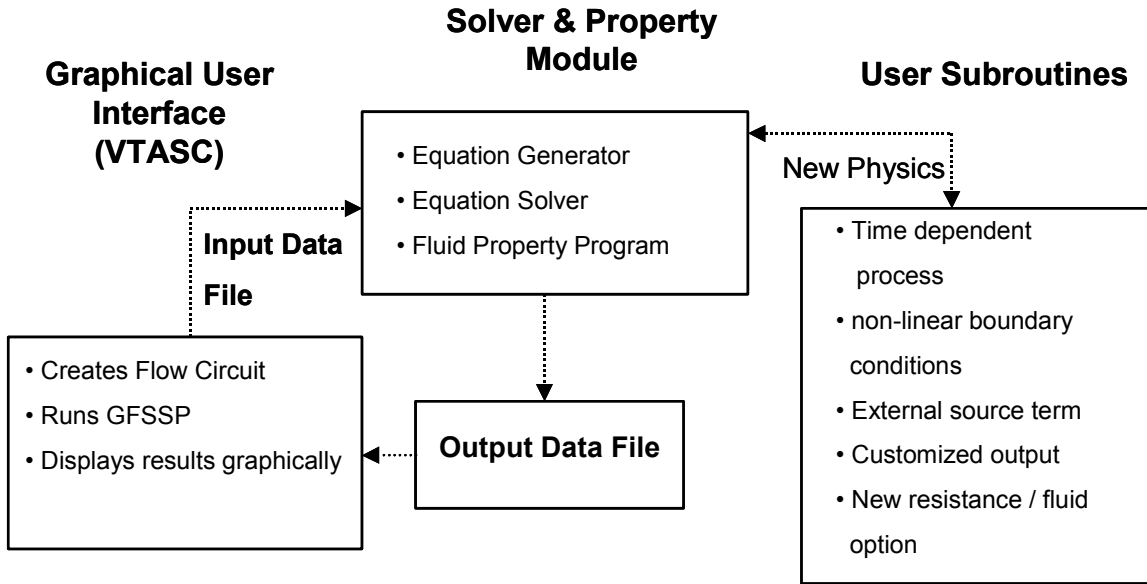


Figure 5. GFSSP Program Structure

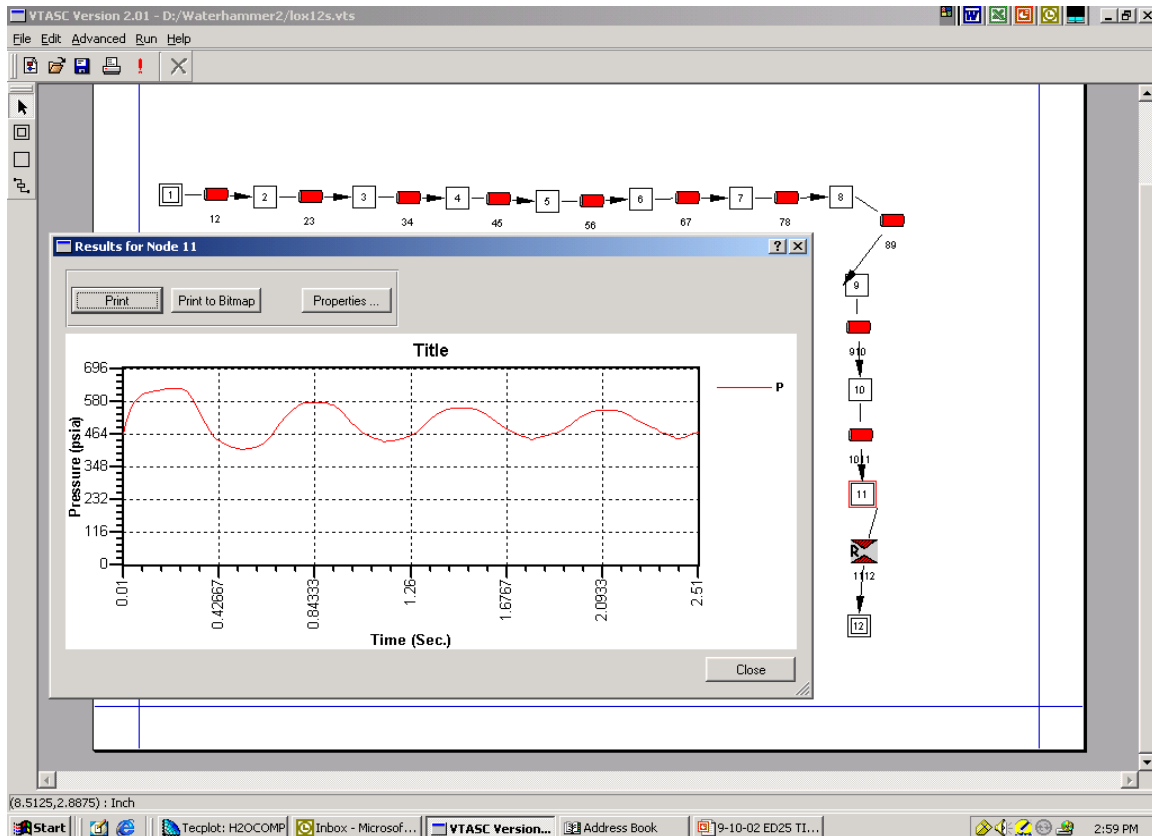


Figure 6. GFSSP's Graphical User Interface, VTASC

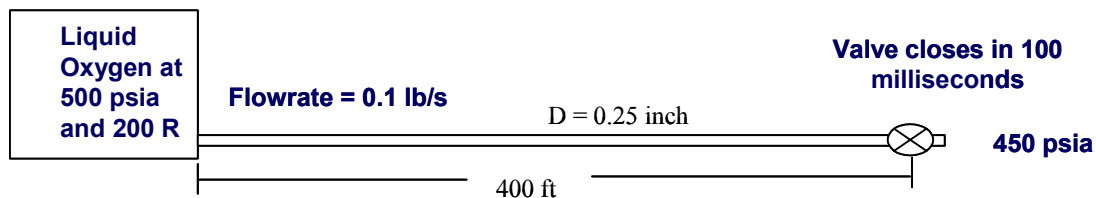
The solver module also interacts with User Subroutines, which are a set of blank subroutines called from solver module. Users can add new physics to the code by writing codes in these subroutines. Typical examples of possible use of User Subroutines include: time dependant boundary conditions, heat and mass transfer from and to surroundings, resistance and fluid options not available in the code.

## RESULTS

Analysis of thermodynamic transients such as blowdown and pressurization was reported in previous publications [11,12]. The purpose of the present paper is to highlight the analysis of fluid transients. Two examples of thermofluid transients are described. In the first example [13], fluid transient after a rapid closing of a valve (commonly known as waterhammer) in a long cryogenic pipeline was calculated and compared with the solution of method of characteristics. In the second example [14], the chilldown of a long cryogenic pipeline was modeled and compared with experimental results.

### Waterhammer

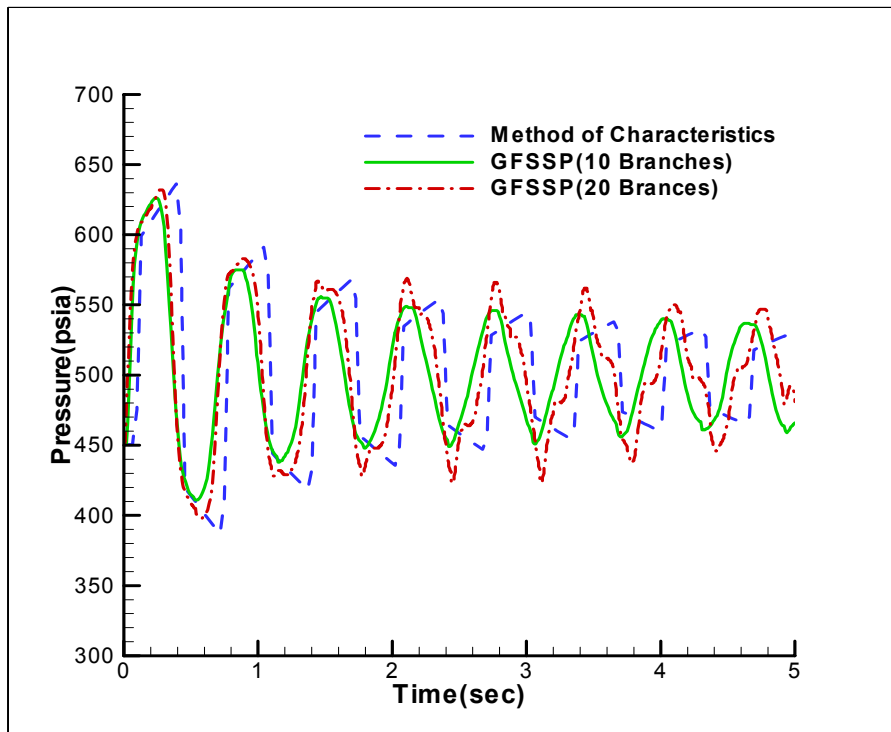
Figure 7 shows a long pipeline connected to a tank. An isolation valve is placed at the end of the pipeline. The valve closes in 0.1 s, which is considered rapid closure since the valve closure time is less than the period of oscillation,  $2L/a$ , where  $L$  is the length of the tube and  $a$  is the speed of sound.



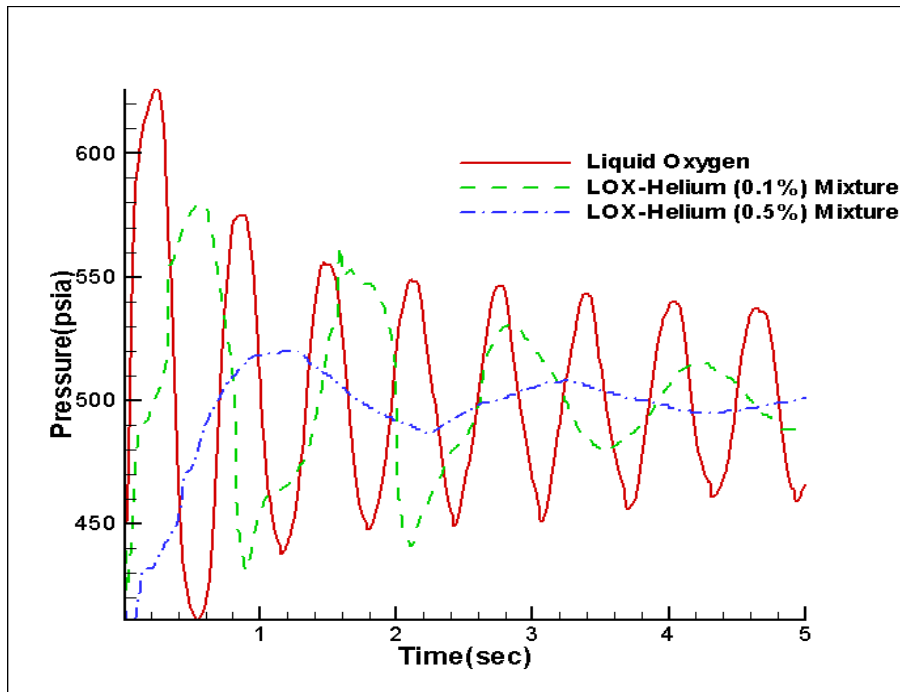
**Figure7. Schematic of the propellant tank, pipeline and valve**

Figure 8 shows comparison between the solution of Method of Characteristics and GFSSP predictions. It is observed that there is a perfect agreement for the period of oscillation between two methods. Both solutions are also in agreement with the characteristic wavelength equation expressed as  $(\lambda = 4L/a)$  where  $\lambda$  is the period of oscillation. Maximum pressure predicted by two methods compares reasonably well. With grid refinement, the GFSSP solution of maximum pressure tends to approach the MOC solution.

Modeling of gas-liquid mixture is demonstrated in Figure 9. The downstream pressure was adjusted until the flowrate nearly matches the case described in Figure 7. With the identical valve closure sequence and 0.1 % by mass of GHe, the peak pressure decreases from 626 to 580 psia and the period of oscillation increases from 0.65 to 1.24 s. With 0.5% mass of GHe, the peak pressure drops to 520 psia and the period of oscillation increases to 2.08 seconds. With the presence of GHe, the compressibility increases; therefore peak pressure decreases.



**Figure 8. Predicted pressure by Method of Characteristics and Finite Volume (GFSSP) Methods**



**Figure 9. Comparison of predicted pressure history for liquid and gas liquid mixtures**

## Chilldown of Cryogenic Transfer Line

This section presents the results of GFSSP model of an experiment performed by the National Bureau of Standards (NBS) [15]. NBS's experimental setup, shown schematically in Figure 10, consisted of a 10.59 ft<sup>3</sup> supply dewar, an inlet valve, and a 200 ft long, 5/8 in inside diameter vacuum jacketed copper transfer line that exhausted to atmosphere.

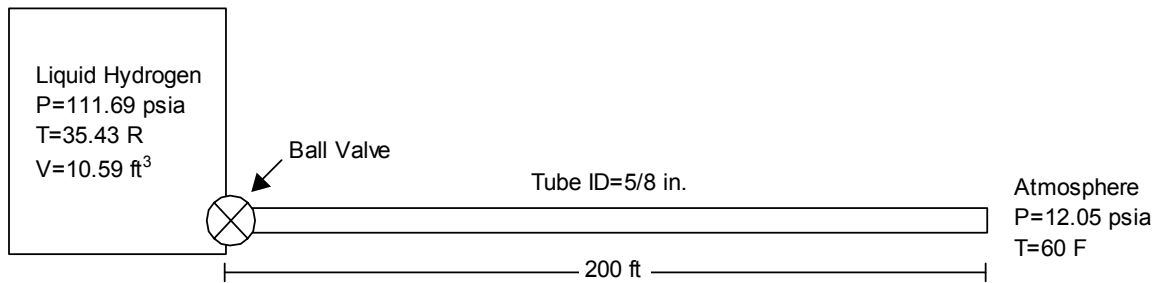


**Figure 10. Hydrogen Line Chilldown Experimental Set-up Schematic**

Figure 11 compares the wall temperatures of the 10- and 30-node transfer line grid resolution predictions of the numerical model and the experimental transfer line wall temperatures published by Brennan et al [15] over the course of a 90-s simulation. Stations 1-4 are nodes whose locations approximately correspond to four instrument stations in the original experimental setup. In the model, the stations are located at 20, 80, 140, and 200 ft, respectively, downstream of the tank. It can be seen by comparing the three cases in Figure 6 that the model's predicted behavior agrees very well, qualitatively, with that observed by Brennan et al. in their experiments. [15] However, the initial second-phase simulations that were performed with a 10-node transfer-line grid resolution predict a chilldown time at Station 1 that is roughly 20 s slower than the experimental data, and a chilldown time at Station 4 that is roughly 23 s slower than that observed by the experiment. This discrepancy led to the decision to increase the transfer-line grid resolution from 10 to 30 nodes. The 30-node transfer-line grid-resolution model predicts a chilldown time at Station 1 that is roughly 8 s slower than the experimental data, and a chilldown time at Station 4 that is roughly 17 s slower than that observed by the experiment. While discrepancies still exist between the predicted and experimental chilldown times, the 30-node transfer-line grid-resolution results show a marked improvement in chilldown prediction time over the 10-node transfer-line grid-resolution model. One reason for the discrepancy in predicted chilldown time is that longitudinal conduction was not accounted for by this model, which can be seen in Figure 11 by noting that the discrepancy in predicted chilldown time increases at each successive station down the length of the transfer line.

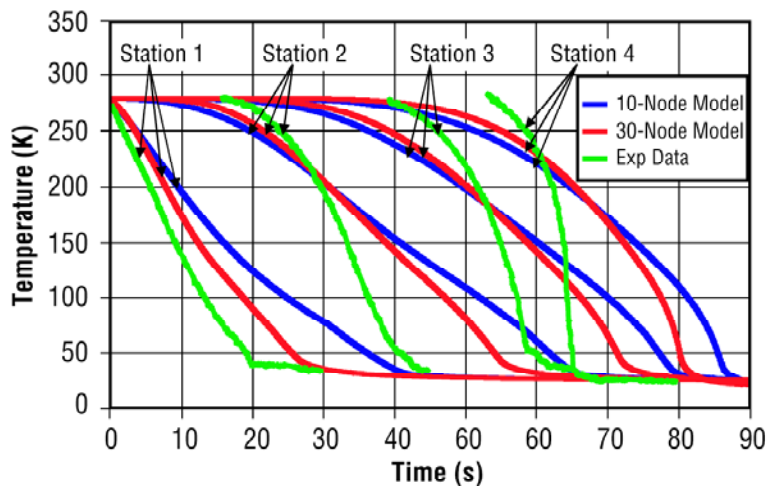


**Figure 12. Comparison of predicted and measured tube wall temperature history**

## CONCLUSIONS

A finite volume based network analysis procedure has been developed to compute fluid transient following rapid valve closure and the chilldown of a long cryogenic transfer line. Liquid has been modeled as compressible fluid where the compressibility factor is computed from the equation of state for a real fluid. The modeling approach recognizes that the pressure oscillation is linked with the variation of the compressibility factor; therefore, the speed of sound does not explicitly appear in the governing equations. It has also been demonstrated that the present procedure can be applied to model fluid transients in a gas liquid mixture. The ability to handle conjugate heat transfer problem was demonstrated by modeling the chilldown of the cryogenic transfer line. It is felt that the inclusion of longitudinal conduction between solid nodes in the numerical model will further increase the accuracy of the model predictions.

## ACKNOWLEDGMENTS

This work has been performed under the MSFC Center Director's Discretionary Fund, Project No. 01-12 and Technology Investment Project No. 02-08. The author would like to acknowledge Eric Stewart of the Thermodynamics and Heat Transfer Group (ED25), MSFC, for his suggestions during the investigation, and Mr. Todd Steadman of Jacobs Sverdrup Technology for engineering support.

## REFERENCES

1. Moody, F. J., Introduction to Unsteady Thermofluid Mechanics, John Wiley & Sons, 1990
2. Wylie, E. B., Streeter, Victor, Fluid Transients, FEB Press, Ann Arbor, MI, 1982.
3. Cullimore, B. A., Goble, R. G., Jensen, C.L., Ring, S. G., "Systems Improved Numerical Differencing Analyzer – 1985 Version with Fluid Integrator (SINDA'85 /FLUINT) User's Manual, Revision 3, Sept. 1988.
4. MSC.EASY5 – Software for virtual system prototyping, simulation, and control, MSC Software.

5. Majumdar, Alok, "Generalized Fluid System Simulation Program (GFSSP) Version 3.0", Report No.: MG-99-290, Sverdrup Technology, Huntsville, Alabama, November, 1999.
6. Colebrook, C. F., "Turbulent Flow in Pipes, with Particular Reference to the Transition Between the Smooth and Rough Pipe Laws", J. Inst. Civil Engineering, London, vol. 11, pp. 133-156, 1938-1939.
7. Patankar, S. V., Numerical Heat Transfer, Hemisphere Publishing Corp., Washington, DC, 1980.
8. Hendricks, R. C., Baron, A. K., and Peller, I. C., "GASP - A Computer Code for Calculating the Thermodynamic and Transport Properties for Ten Fluids: Parahydrogen, Helium, Neon, Methane, Nitrogen, Carbon Monoxide, Oxygen, Fluorine, Argon, and Carbon Dioxide", NASA TN D-7808, February, 1975.
9. Hendricks, R. C., Peller, I. C., and Baron, A. K., "WASP - A Flexible Fortran IV Computer Code for Calculating Water and Steam Properties", NASA TN D-7391, November, 1973.
10. Miropolskii, Z.L.: "Heat Transfer in Film Boiling of a Steam-Water Mixture in Steam Generating Tubes," *Teploenergetika*, Vol. 10, 1963, pp. 49-52; transl. AEC-tr-6252, 1964.
11. Majumdar, A. K., "A Second Law Based Unstructured Finite Volume Procedure for Generalized Flow Simulation", Paper No. AIAA 99-0934, 37<sup>th</sup> AIAA Aerospace Sciences Meeting Conference and Exhibit, January 11-14, 1999, Reno, NV.
12. Majumdar, A. K. and Steadman, T., "Numerical Modeling of Pressurization of a Propellant Tank", Journal of Propulsion and Power, Vol. 17, No. 2, 2001, pp. 385-390.
13. Majumdar, Alok, and Flachbart, R.H., "Numerical Modeling of Fluid Transient by a Finite Volume Procedure for Rocket Propulsion Systems," Proceedings of ASME FEDSM'03, 4<sup>th</sup> ASME/JSME Joint Fluids Engineering Conference, Paper No. FEDSM2003-45275, Honolulu, Hawaii, USA, July 6-10, 2003.
14. Majumdar, Alok, and Steadman, Todd, "Numerical Modeling of Thermofluid Transients During Chillydown of Cryogenic Transfer Lines" 33<sup>rd</sup> International Conference on Environmental Systems (ICES), Paper No. 2003-01-2662, Vancouver, Canada, July 6-10, 2003.
15. Brennan, J.A.; Brentari, E.G.; Smith, R.V.; and Steward, W.G.: "Cooldown of Cryogenic Transfer Lines—An Experimental Report," Report No. 9264, National Bureau of Standards, November 1966.

## NOMENCLATURE

A	Area (in <sup>2</sup> )
a	Speed of Sound (ft/sec)
C <sub>L</sub>	Flow Coefficient
c <sub>i,k</sub>	Mass Concentration of k <sup>th</sup> Specie at i <sup>th</sup> Node
C <sub>p</sub>	Specific Heat at constant pressure (Btu/lb °F)
C <sub>v</sub>	Specific Heat at constant volume (Btu/lb °F)
D	Diameter (in)

f	Friction Factor
GHe	Gaseous Helium
$g_c$	Conversion Constant (= 32.174 lb-ft/lb <sub>f</sub> -sec <sup>2</sup> )
h	Enthalpy (Btu/lb)
J	Mechanical Equivalent of Heat (= 778 ft-lb <sub>f</sub> /Btu)
$K_f$	Flow Resistance Coefficient (lb <sub>f</sub> -sec <sup>2</sup> /(lb-ft) <sup>2</sup> )
L	Length (in)
M	Molecular Weight
LO <sub>2</sub>	Liquid Oxygen
m	Resident Mass (lb)
$\dot{m}$	Mass Flow Rate (lb/sec)
N <sub>E</sub>	Number of Iterations
Nu	Nusselt number
n <sub>f</sub>	Number of fluids in a mixture
p	Pressure (lb <sub>f</sub> /in <sup>2</sup> )
Pr	Prandtl number
$\dot{Q}$	Heat transfer rate (Btu/s)
R	Gas Constant (lb <sub>f</sub> -ft/lb-R)
Re	Reynolds Number
T	Temperature (° F)
u	Velocity (ft/sec)
V	Volume (in <sup>3</sup> )
x <sub>v</sub>	Vapor Quality
x	Mass Fraction
$\bar{x}$	Mole Fraction
z	Compressibility Factor

### Greek

$\rho$	Density (lb/ft <sup>3</sup> )
$\mu$	Viscosity ( lb/ft-sec)
$\Delta\tau$	Time Step (sec)
$\tau$	Time (sec)
$\varepsilon$	Surface Roughness of pipe (in)

### Subscript

i	Node
ij	Branch
k	Specie
f	Liquid
g	Vapor